



Fabrication of Paper-Templated Structures of Noble Metals

Citation

Christodouleas, Dionysios C., Felice C. Simeone, Alok Tayi, Sonia Targ, James C. Weaver, Kaushik Jayaram, Maria Teresa Fernández-Abedul, and George M. Whitesides. 2017. "Fabrication of Paper-Templated Structures of Noble Metals." *Advanced Materials Technologies* 2 (2) (January 11): 1600229. doi:10.1002/admt.201600229.

Published Version

10.1002/admt.201600229

Permanent link

<http://nrs.harvard.edu/urn-3:HUL.InstRepos:34708433>

Terms of Use

This article was downloaded from Harvard University's DASH repository, and is made available under the terms and conditions applicable to Open Access Policy Articles, as set forth at <http://nrs.harvard.edu/urn-3:HUL.InstRepos:dash.current.terms-of-use#OAP>

Share Your Story

The Harvard community has made this article openly available.
Please share how this access benefits you. [Submit a story](#).

[Accessibility](#)

Fabrication of Paper-templated Structures of Noble Metals

Dionysios C. Christodouleas¹, Felice C. Simeone¹, Alok Tayi¹, Sonia Targ¹, James C. Weaver²,
Maria Teresa Fernández-Abedul³, George M. Whitesides^{1,2*}

¹Department of Chemistry and Chemical Biology, Harvard University, Cambridge, MA, United States

²Wyss Institute for Biologically Inspired Engineering, Harvard University, Cambridge, MA, United States

³Departamento de Química Física y Analítica, Universidad de Oviedo, Asturias, Spain

* Corresponding author E-mail: gwhitesides@gmwgroup.harvard.edu

Introduction

Noble metals find application in a variety of fields, including electroanalysis [1] and electrocatalysis [2]. To form electrodes, bulk metals are shaped into rods, or into thin films supported on flat substrates (e.g., ceramic materials, glass) [3,4]; thin films may be roughened to increase their surface areas [2]. Alternatively, metal nanoparticles are deposited on a high-surface, inexpensive supporting electrode (e.g., carbon [1]). Electrodes composed of bulk noble metals do not provide high surface area per unit of weight of metal; in addition, they are not permeable to gases and liquids. Electrodes composed of metal nanoparticles can have high surface area per unit of weight of metal, but may (depending on the support) be impermeable to gases and liquids.

Papers and fabrics have open fibrous structures, which provide them with higher accessible surface area than flat films of similar dimensions; they are also permeable to liquids and gases. If noble metals could be fabricated in structures that are morphologically similar to paper or fabric, these structures might exhibit attractive physical properties (e.g., high surface area, mechanical flexibility, permeability to gases and liquids) and be plausible materials for use in electroanalysis, as catalysts or electrical conductors, or magnetic collectors.

This article describes a method for fabricating free-standing materials of a number of late transition metals; these materials have physical morphologies that resembles paper, thread, or fabric. This method uses paper or fabric as a template, and solutions of metallic ions as precursors to the metal. We call the method “paper-templating”, and the resulting structures “paper-templated metals.” In this method, the template is first loaded with aqueous solutions of salts of noble metals and dried; the template is then burned off in a furnace held at temperatures between 550 °C to 800 °C, depending on the procedure, and the resulting structure annealed for two minutes. The method yields structures composed primarily (> 94 % w/w) of elemental metal; these structures resemble the shape of the original template (Figure 1A-B) and have a morphology, at scales down to 2 μm , similar to that of the material (e.g., paper) from which they were derived (Figure 1C-F). Using paper-templating, we fabricated: i) paper-templated structures of noble metals (i.e., gold, silver,

platinum, rhodium, palladium, and iridium), ii) paper-templated structures of mixtures or alloys of noble metals (i.e., gold-platinum, silver-palladium, gold-rhodium and gold-rhodium-platinum), and iii) paper-templated structures with different regions composed of a different noble metal (i.e., gold/silver, platinum/rhodium). These structures exhibited high electrical conductivity, and permeability to gases and liquids. The surface areas of these structures were more than 20 times higher than the projected area. The surface of paper-templated gold was electroactive, and the structure could be used as the working electrode for electroanalysis (Figure 1G-H).

Previous efforts to prepare porous structures of noble metals have used methodologies that were based on i) packed colloidal spheres used as templates [5-10], ii) replacement reaction between a silver template and the salt solution of a metal (whose redox potential, M^{n+}/M , was higher than that of the Ag^+/Ag couple, as, for example, Au) [11,12], and iii) selective dissolution of a metal from a film of metal alloy [13-16]. Although these and similar techniques can provide films or nanostructures with well-defined nanopores, they require complicated experimental procedures [9,10] and produce either nanostructures [11], or very thin (on the order of a few microns) and fragile films [9,10]. For example, Velev and coworkers used templates of colloidal spheres to prepare flakes of nanoporous gold with projected areas not bigger than 2 mm^2 [5]. Xia and coworkers synthesized aggregates of nanostructures of gold, platinum, and palladium with hollow interiors using, as templates, silver nanoparticles of various morphologies, and solutions of gold, platinum, or palladium salts as precursors to the metals [11]; in this method, metal ions (i.e., Au^{3+} , Pt^{4+} , Pd^{2+}) were reduced on the surface of silver nanoparticles, and an elemental metal (i.e., Au, Pt, Pd) grew into a shell-like structure, while silver nanoparticles were simultaneously oxidized to soluble silver ions [11]. Alternatively, nanoporous thin films of gold can be prepared by dissolving silver from a film of a silver-gold alloy [13].

Other methods used carbon-based polymeric materials, such as paper and polymeric fibers, as templates for the fabrication of porous structures of metal oxides (e.g., TiO_2 , MnO_2 , Fe_2O_3) [17-21]. Yuan *et al.* prepared hollow metal oxide fibers composed of TiO_2 or Fe_2O_3 by coating carbon

fibers with solutions of precursors of the metal oxides, and then removing the carbon fibers by oxidation [17]. Kunitake and coworkers prepared paper-templated films of TiO_2 by heating from room temperature to 450 °C, in air, filter paper loaded with titanium butoxide [21]. They attempted to use the same approach also to prepare a paper-templated structure of silver, using solutions of AgNO_3 , but they produced, instead, a metallic powder of silver [22]; they fabricated a free-standing structure of silver fibers only after using sodium borohydride to reduce the silver ions to silver, and then burning the paper to fuse the silver nanoparticles together. These structures had morphology similar to that of paper, but their shapes were irregular [22].

RESULTS AND DISCUSSION

Fabrication of the Structures. This work describes a method to prepare free-standing paper-templated structures of most of elements considered to be noble metals (i.e., gold, silver, platinum, rhodium, palladium, and iridium). We fabricated the structures as follows: We used templates made of Chromatography Paper Grade A, and defined the hydrophilic region of each template by printing hydrophobic barriers composed of wax-based ink. We then added onto the hydrophilic region a salt solution of metallic ions (e.g., for the gold structure $\sim 7.5 \text{ mg-atom} / \text{cm}^2$ for chromatography paper 180- μm thick. The supporting Information reports the exact concentration and volume of salt solution used for each structure.) We let water evaporate from the paper template at 70 °C. After the paper template dried, we cut off the hydrophobic barriers and placed it between two flat layers of stainless steel mesh. The template was then placed in a furnace pre-heated to high temperatures (i.e., from 550 °C to 800 °C, depending on the procedure) in air. Inside the furnace, the template auto-ignited and the paper burned off within a few seconds, yielding a paper-templated metallic structure. We left this structure in the furnace for two minutes to anneal, and then we let it cool to room temperature. We carefully removed one layer of the stainless steel mesh and retained the paper-templated metallic structure (Figure S-1.)

The composition of the solution applied to the original template determined the final composition of the metallic structure. By using solutions containing a mixture of metallic ions, we prepared paper-templated structures composed of i) gold and platinum (Au-Pt), ii) silver and palladium (Ag-Pd), iii) gold and rhodium (Au-Rh), and iv) gold, rhodium and platinum (Au-Rh-Pt) (Figure S-1.) The detailed experimental procedure is described in the Supporting Information. We also prepared paper-templated structures with each half of the structure composed of a different noble metal (i.e., gold and silver (Au/Ag), and platinum and rhodium (Pt-Rh)) (Figure 2A-B); these structures were generated by wetting the two halves of a rectangular paper template with separate solutions containing different metal ions (see Supporting Information for the experimental procedure.) Figure 2C-F shows that each half of the structure was composed primarily of a single metal with only partial mixing at the interface between them. There are two plausible reasons for the segregation of the metals [23]. i) Once the two solutions of metallic ions met in the middle of the rectangular template, capillarity-driven flow of liquid through the paper stopped. ii) Diffusion of metallic ions, due to concentration gradients across the interface between the two liquids, occurred only on the scale of a millimeter before water evaporated completely (Figure 2E-F).

Physical Properties and Morphology of Paper-templated Structures. Paper-templating generated structures that were free-standing and almost flat (with wrinkles mainly due to the warping of the structure that occurred during the combustion of the cellulose). The shape of the structures could be tailored by using templates of different shapes; Figure S-2 shows paper-templated structures made of gold, silver, platinum, and rhodium that have triangular, square, rectangular and circular shapes depending on the shape of the original structure.

All of the paper-templated structures were flexible, with the exception of those composed of iridium and palladium, which were fragile and brittle. Among the samples we fabricated, the paper-templated structures of silver were the most robust: they remained intact even when we creased, or scrolled them (Figure S-3.)

To test whether the paper-templated structures were permeable to liquids, we placed gold or silver paper-templated structures between two sheets of paper, pressed them, and added a drop of water on top of one layer of paper. Water wicked slowly through the paper-templated structures to the bottom piece of paper.

The footprint areas of the metallic structures were smaller than those of the original templates by at least a factor of 1.5 (Figure S-1, and S-2.) The projected areas of rhodium and platinum structures were ~ 0.6 of the areas of the original templates. For gold structures, the projected area of the paper-templated structures was ~ 0.3 that of the area of the original template. The mean thickness of the structures was between 50 and 150 μm , depending on the metal used (Table S-1.) The average thickness of the silver structures was $150 \pm 20 \mu\text{m}$ ($N=5$), while the average thickness of the iridium structure was $50 \pm 4 \mu\text{m}$ ($N=5$). (The thickness of the native chromatography paper was 180 μm .)

To the naked eye, the paper-templated structures appeared fibrous and porous. Scanning Electron Microscopy (SEM) confirmed that the structures were composed of metallic fibers that, remarkably, were interconnected and formed a continuous network that resembled that of the paper from which they were derived (Figures 1C-F, Figure S-4, and Figure S-5.) The diameter of the metallic fibers ranged from 2 to 10 μm . The dimensions and the morphologies of the metallic fibers were influenced by i) the amount of the metallic ion used as precursor and deposited on the template (Figure S-6), and ii) the noble metal. For example, gold and silver fibers appeared solid, while the platinum ones appeared porous (Figures 1F, S-4B and S-4D.)

Because they were fibrous and porous, the paper-templated structures had surface areas that were higher than the projected areas. We measured the specific surface area (using a multipoint Brunauer, Emmett and Teller (BET) method; krypton was used as adsorbate gas) of the gold, silver, and platinum paper-templated structures (Table 1). For comparison, we also measured the specific surface area of the original paper used as the template and that of a 0.025-mm-thick gold foil (Table 1). The paper-templated metallic structures had an area that was ~ 0.2 of the area of the paper, but

~15 times that of the thin gold metal foil, and more than 20 times that of the projected area of the structure. We mention, for comparison, that Hu *et al.* prepared nanoporous gold structures (by dissolving silver from a silver/gold alloy) that had surface areas 9.2 times larger than that of a flat structure [24]. Preliminary results on the paper-templated gold structures suggested that we could prepare paper-templated metallic structures of even higher surface area ($\sim 1 \text{ m}^2/\text{g}$ or $\sim 256 \text{ m}^2/\text{g-atom}$) by reducing the amount of metal precursor added on the paper template, these structures, however, were fragile. Other structures (i.e., exfoliated graphite, mesoporous alumina) reported in the literature [25,26] exhibited much higher surface area than paper-templated structures (Table 1), but they were not free standing.

Characteristics and Composition of Paper-templated Structures. The color of each paper-templated structure (Figures S-1, and S-2) matched the color of the elemental metal of which it was composed. We calculated the composition of each structure using Energy Dispersive Spectroscopy (EDS): EDS estimated the composition of the outer parts of the paper-templated structures (less than $2 \mu\text{m}$ inside the body of the fiber.) In all structures, the mass percentage of the target noble metals exceeded 94% while the mass percentages of carbon and oxygen in the structures were below 6% (Table 2). We also performed depth-profile X-ray photoelectron spectroscopy (XPS) experiments and we concluded that in all structures carbon and oxygen were present mainly on the surface of the structure (in the upper few nanometers). Specifically, we removed 10 nm of the surface material by sputtering argon and we measured the composition of the new surface of the metallic structures. In all structures the atomic percentage of carbon and oxygen in the structures were significantly reduced compared to those of the initial surface of the structures (Table S-2.) We therefore concluded that i) the noble metals were mainly in elemental form; EDS results show that, in all cases, the atomic percentage of oxygen in the structures was less than half that of the noble metal; this ratio implies that metal oxides, although present in the surface, were not the main components of the structures; ii) oxygen was part of metal oxides that formed at the surface of the metallic

fibers probably during cooling to room temperature; for example, platinum, iridium and rhodium form oxides when heated in presence of oxygen [27]), iii) carbon is in elemental form, which, we presume, derived from the residual soot that formed during the combustion of the paper template; we infer that carbon did not result from the formation of carbides of noble metals because they are unstable and require more extreme conditions (e.g., during laser ablation or laser desorption processes) than those used here [28].

Electrical Properties of Paper-templated Structures. The paper-templated metallic structures were electrically conductive and exhibited a linear variation (Ohmic behavior) of the electrical current with the applied voltage. The apparent volume resistivities of these structures, however, were ~ 1000 times higher than those of sheets of pure metals (Table 3) [29], perhaps for four reasons: i) the electrical path within each structure was longer (the exact length was actually unknown) than the length of the structure, ii) the resistance associated with the oxides and impurities found in the structures contributed to their resistance, iii) the contact resistance at points where current passed from one fiber to the next was high; and iv) the constriction resistance (i.e., the resistance associated to the flow of the current through volumes much smaller than the average volume of the sample) added to the other sources of resistance. Constriction resistance originates mainly at point contacts between fibers, and at regions of the fibers of irregular thickness; constriction resistance can dominate the resistance of an entire sample, especially when the sample is composed of a highly conductive material [30].

Paper-templated Electrodes in Electrochemical Cells. Noble metals are often used for the fabrication of electrodes for electroanalytical measurements, and for electrocatalysis. To test the performance of paper-templated gold and platinum structures (which were permeable to liquids) as electrodes in an electrochemical cell, we recorded cyclic voltammograms in 5-mM solutions of

$\text{Fe}(\text{CN})_6^{4-}$ at scan rates between 10 and 150 mV/s (Figure S-7.); the $\text{Fe}(\text{CN})_6^{4-}/\text{Fe}(\text{CN})_6^{3-}$ couple is a well-characterized reversible redox system commonly used as a model system [31].

For both paper-templated gold and platinum electrodes the $\text{Fe}(\text{CN})_6^{4-}/\text{Fe}(\text{CN})_6^{3-}$ couple exhibited a quasi-reversible behavior; the values of the ratio of the anodic to cathodic peak current ($i_{\text{pa}}/i_{\text{pc}}$), in fact, were slightly higher than unity, and the separation of peak potentials ($E_{\text{pa}} - E_{\text{pc}}$) exceeded, at all scan rates, 59 mV (Figure S-8A to Figure S-8D), which is the separation between anodic and cathodic peak potentials expected for reversible redox process under the assumption of planar diffusion [32]. The values of the logarithm of anodic peak current varied linearly with the logarithm of scan rate (Figure S-8E, Figure S-8F), but with a slope greater than 0.5, which is the value predicted by the Randles-Sevcik equation assuming planar diffusion of the redox species toward, and away from, the electrode [32]. This equation, in fact, assumes that the electrodes are flat, and that the diffusion layers of the redox reagents are semi-infinite [32], two conditions that are not met by paper-templated electrodes, which are porous with the pore size varying significantly from several nanometers to a few micrometers. We, therefore, conclude that for paper-templated electrodes mass transport deviated from planar diffusion: if gradients in patterns of diffusion occur in different regions of a paper-templated electrode at the same time, it will be difficult to express the measured currents using an equation similar to the Randles-Sevcik equation [33].

From the capacitive currents recorded in the voltammograms, we estimated an electrochemically active surface area of 0.025 m²/g for gold, and of 0.105 m²/g for platinum, paper-templated structures (see Supporting Information for details.) The electrochemically active surface area of the paper-templated structures was < 0.14 that of the surface area estimated by the BET method. Two plausible origins of the difference are: i) krypton gas could reach areas of the structures (e.g., small pores) that were not accessible to solutions, and ii) non-metallic (or non-conductive) components of the electrodes and perhaps impurities on their surfaces reduced the electrochemically active surface area.

We used paper-templated gold as the working electrode in an electrochemical cell used for electroanalysis. To calibrate the electrochemical response of the electrode, we recorded cyclic voltammograms in solutions of $\text{Fe}(\text{CN})_6^{4-}$ at different concentrations (i.e., 0.5-10 mM) (Figure 1G). Figure 1H shows that the average intensity of the peak currents varied linearly with the concentration of $\text{Fe}(\text{CN})_6^{4-}$, and reproducibility was adequate for routine electroanalysis.

Fabric-templated and Sponge-templated Structures. To demonstrate the applicability of paper-templating to the fabrication of structures with morphology more complex than non-woven paper, we prepared structures template by cotton lace and woven fabric (Figure 3, S-9, and S-10A to S-10D). Figure 3 shows that lace-templated silver structure retained the woven morphology of the lace template to a remarkable extent.

We also fabricated non-planar, three-dimensional metallic structures by using urethane sponges as templates. These sponge-templated silver structures retained the porosity and the general morphology of sponges (Figure S-10E, and S-10F.)

Mechanism of the Reduction of Metal Ions. While previous studies have examined the chemical reactions that occur during the combustion of paper [34], the exact set of chemical reactions and intermediate products, especially during oxidation with an active flame that leads to the paper-templated structures of noble metals we have observed, are not known.

We propose two possible mechanisms for the reduction of noble metal ions deposited on the surface of the template. i) One possibility is that they result from the reduction of metal ions to elemental metals by carbon monoxide and hydrogen formed during the combustion of paper. In the present study, we incinerated the paper templates at temperatures and atmospheres similar to those used by Cullis *et al* for the combustion of cellulose (at 550 °C in atmospheres containing 21% v/v oxygen and 79% v/v nitrogen); those combustion experiment yielded carbon monoxide (7.3 mmol/L), carbon dioxide (5.8 mmol/L), and hydrogen (1.2 mmol/L) [35]. At high temperatures,

carbon monoxide and hydrogen are both strong reducing agents; carbon monoxide, in fact, is typically used in metallurgy for the reduction of Fe_2O_3 to elemental iron in a blast furnace [36]. We believe that, in proximity to the burning paper, the concentration of carbon monoxide and hydrogen may be high enough to reduce metal ions to elemental noble metal; Ellingham diagrams suggest that, under specific experimental conditions (i.e., temperature, $p\text{O}_2$, $p\text{CO}$, $p\text{CO}_2$, $p\text{H}_2$), the free energy of the reaction of carbon monoxide and hydrogen with oxides of noble metals is negative and, therefore, thermodynamically favorable (Figure S-11.) [37] ii) The second possibility is that metallic paper-templated structures result from the thermal decomposition of salts of noble metals to elemental metals at high temperatures. When dried on paper, salt solutions of noble metals ions crystallized as salts. Salts of noble metals, however, are unstable at high temperatures and can decompose through several routes to elemental metal. For example, AgNO_3 decomposes in the temperature range of 360–515 °C to Ag, NO_2 , NO and O_2 [38]. The combustion of paper releases heat that increases the temperature of the template above that of the furnace; based on the color of the burning template inside the furnace (the color was red to orange), we estimated that the actual temperature of the burning template can reach ~850 °C. These temperatures may be high enough, in some cases, to cause the decomposition of the salts to clusters of elemental metal (e.g., to elemental silver). RhCl_3 , however, decomposes between 650-750 °C to Rh_2O_3 , which, in turn, decomposes to elemental Rh only at 1040-1060 °C. [39] IrCl_3 decomposes between 500-680 °C to IrO_2 , and then to elemental Ir at 1025-1070 °C [39].

Fabrication of Conductive Silver Lines Using a Laser Cutter. To generate paper-templated silver wires of arbitrary shapes embedded in, and on, paper, (Figure 4) we used the laser beam found in a commercial laser cutter. The laser beam could precisely burn the template locally, and therefore induce the reduction of the silver ions to form 100- μm wide lines (Supporting Information describes the details of this procedure.) Although fragile when they were creased or bent significantly, the lines produced by the laser beam were electrically conductive; we measured the electrical resistance

of the wires to be $\sim 250 \text{ } \Omega/\text{cm}$. This value was similar to electrical resistance measured by Jessing and co-workers for printed silver lines on different types of hydrophobic paper (100 and $400 \text{ } \Omega/\text{cm}$) [40]. Due to its simplicity, we believe that our method, after further modifications and optimizations, might be used as an alternative method to the fabrication of conductive wires.

Conclusion

This paper describes a convenient and rapid method to prepare paper-templated and fabric-templated structures composed of noble metals. The composition of these paper-templated substrates can be varied by changing the composition of the solutions of the precursors. The shape of the paper-templated structures can be also tailored by changing the shape of the original template. The retention of shape in going from the original paper template to metal structure is however, only approximate. Achieving better retention—with less shrinkage and warping—would be required for applications requiring specific, complex shapes.

Although this study has focused on the fabrication of structures composed mainly of noble metals, this method can be used also for the fabrication of metal oxide structures. For example, by using solutions of TiCl_3 and AlCl_3 as precursors, we produced paper-templated structures composed of TiO_2 , and Al_2O_3 (Figure S-12.) The method is generally much faster than others described in the literature, as it requires only a few minutes (compared to few hours) to accomplish [21].

Other porous structures that were made of noble metals, and exhibited high surface areas, have the potential to serve as electrodes in electrochemical sensors and biosensors [41], as well as in catalysis (e.g., for the oxidation of organic molecules (such as methanol, formic acid) [42], and for oxygen reduction reactions used in fuel cells [43]). The paper-templated structures we prepared are fibrous, conductive, possess high surface area, and are gas and liquid permeable. They thus have properties that make them potentially useful in catalysis, sensing, and electroanalysis.

Acknowledgements

The authors wish to acknowledge the Defense Threat Reduction Agency (award number HDTRA1-14-C-0037) for salary support to DC, the Department of Energy award DE-SC00000989 for salary support to FS, the Army Research Office award N00014-10-1-0942 for salary support to AT, the National Science Foundation (award No. DMR-0820484) for salary support to ST, the University of Oviedo (Campus de Excelencia Internacional) and the Spanish Ministry of Economy and Competitiveness (project MICINN CTQ2011-25814) for support to MTFA. They also want to thank Dr. Alar Ainla for taking the photos of the structures, Dr H. Greg Lin for performing the XPS experiments, and Dr. Baris Unal for useful discussions.

References

- [1] C. M. Welch, R.G. Compton, *Anal. Bioanal. Chem.* **2006**, 384, 601.
- [2] A.J. Arvia, R.C. Salvarezza, W.E. Triaca, *J. New. Mat. Electrochem. Systems* **2004**, 7, 133.
- [3] R. Garcia-Gonzalez, M. T. Fernandez-Abedul, A. Pernia, A. Costa-Garcia, *Electrochim. Acta*, **2008**, 53, 3242.
- [4] S. Kishioka, J. Nishino, H. Sakaguchi, *Anal. Chem.* **2007**, 79, 6851.
- [5] O. D. Velev, P. M. Tessier, A. M. Lenhoff, E.W. Kaler, *Nature*. **1999**, 401, 548.
- [6] O. D. Velev, E.W. Kaler, *Adv. Mater.* **2000**, 12, 531.
- [7] P. Jiang, J. Cizeron, J. F. Bertone, V. L. Colvin, *J. Am. Chem. Soc.* **1999**, 121, 7957
- [8] K. M. Kulinowski, P. Jiang, H. Vaswani, V. L. Colvin, *Adv. Mater.* **2000**, 12, 833.
- [9] J. E. G. J. Wijnhoven, S. J. M. Zevenhuizen, M. A. Hendriks, D. Vanmaekelbergh, J. J. Kelly, W. L. Vos, *Adv. Mater.* **2000**, 12, 888.
- [10] H. Xu, W. A. Goedel, *Small* **2005**, 1, 808.
- [11] Y. Sun, B.T. Mayers, Y. Xia, *Nano Lett.* **2002**, 2, 481.
- [12] Y. Sun, B.T. Mayers, Y. Xia, *Adv. Mater.* **2003**, 15, 641.
- [13] J. Erlebacher, M. J. Aziz, A. Karma, N. Dimitrov, K. Sieradzki, *Nature* **2001**, 410, 450.
- [14] Li, R.; Sieradzki, K. *Phys. Rev. Lett.* **1992**, 68, 1168.
- [15] Y. Ding, J. Erlebacher, *J. Am. Chem. Soc.* **2003**, 125, 7772.
- [16] Y. Ding, Y.-J. Kim, J. Erlebacher, *Adv. Mater.* **2004**, 16, 1897.
- [17] R. Yuan , X. Fu , X. Wang , P. Liu , L. Wu , Y. Xu , X. Wang , Z. Wang, *Chem. Mater.*, **2006**, 18 (19), 4700.
- [18] Y. Sun, X. Hu, J. C. Yu, Q. Li, W. Luo, L. Yuan, W. Zhang, Y. Huang, *Energy Environ. Sci.* **2011**, 4, 2870.
- [19] L. Zhou, J. He, J. Zhang, Z. He, Y. Hu, C. Zhang, H. He, *J. Phys. Chem. C* **2011**, 115, 16873.
- [20] B. Zhao, Z. Shao, *J. Phys. Chem. C* **2012**, 116, 17440.
- [21] J. Huang, T. Kunitake *J. Am. Chem. Soc.* **2003**, 125, 11834.
- [22] J. He, T. Kunitake, T. Watanabe, *Chem. Commun.*, **2005**, 6, 795.
- [23] W. Lan, E. J Maxwell, C Parolo, D.K. Bwambok, A. B. Subramaniam, G M. Whitesides, *Lab Chip*, **2013**, 13, 4103.
- [24] K. Hu, D. Lan, X. Li, S. Zhang, *Anal. Chem.*, **2008**, 80, 9124.
- [25] O. N. Shornikova, E. V. Kogan, N. E. Sorokina, V. V. Avdeev, *Russ. J. Phys. Chem. A* **2009**, 83(6), 1022.
- [26] W.-C. Li, A.-H. Lu, W. Schmidt, F. Schuth, *Chem. Eur. J.* **2005**, 11, 1658.
- [27] J. C. Chaston, *Platinum Metals Rev.*, **1975**, 19(4), 135.

- [28] J. Havel, E. M. Peña-Méndez, F. Amato, N. R. Panyala, V. Buršíková, *Rapid Commun. Mass Spectrom.*, **2014**, 28, 297.
- [29] G. T. Meaden, *Electrical Resistance of Metals*, Springer LLC, New York **1965**, p. 4
- [30] J A. Greenwood, *Brit. J. Appl. Phys.* **1966**, 17, 1621.
- [31] A. Nemiroski, D. C. Christodouleas, J. W. Hennek, A. A. Kumar, E. J. Maxwell, M. T. Fernández-Abedul, G. M. Whitesides, *Proc. Natl. Acad. Sci. USA* **2014**, 111, 11984.
- [32] A.J. Bard, L. R. Faulkner, *Electrochemical Methods: Fundamentals and Applications*, Wiley-VCH, Weinheim, Germany, **2000**.
- [33] K. Ngamchuea, S. Eloul, K. Tschulik, R. G. Compton, *J Solid State Electrochem.*, **2014**, 18, 3251.
- [34] D. K. Shen, S. Gu, *Bioresource Technol.*, **2009**, 100, 6496.
- [35] C. F. Cullis, M. M. Hirschler, R. P. Townsend, V. Visanuvimol, *Combust. Flame*, **1983**, 49, 249.
- [36] K. Li, R. Khanna, J. Zhang, Z. Liu, V. Sahajwalla, T. Yang, D. Kong, *Fuel*, **2014**, 133, 194.
- [37] T. Reed, *Free Energy of Formation of Binary Compounds*, MIT Press, Cambridge MA, **1971**
- [38] K. Otto, I. Oja Acik , M. Krunks, K. Tönsuaadu, A. Mere, *J. Therm. Anal. Calorim.*, **2014**, 118, 1065
- [39] A.E Newkirk and D.W. McKee, *J. Catal*, **1968**, 11, 370
- [40] J. Lessing, A.C. Glavan, S.B. Walker, C. Keplinger, J.A. Lewis, G.M. Whitesides. *Adv. Mater.* **2014**, 26, 4677.
- [41] A. Walcarius, A. Kuhn, *TrAC-Trend Anal. Chem.*, **2008**, 27, 593.
- [42] J. Zhang, C.M. Li, *Chem. Soc. Rev.*, **2012**, 41, 7016.
- [43] Y. Qiao, C.M. Li, *J. Mater. Chem.*, **2011**, 21, 4027.

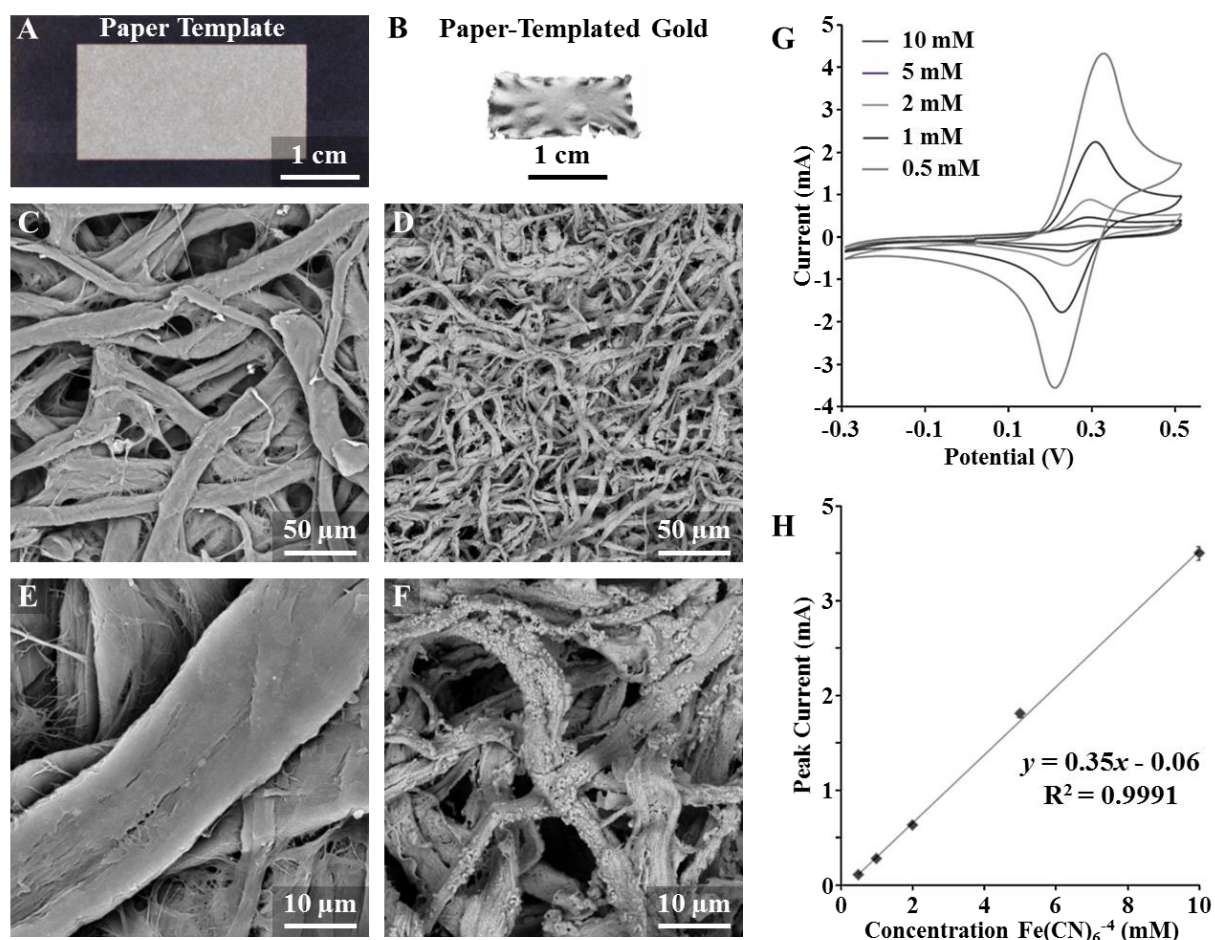


Figure 1. Photographs of the paper template (A) used to produce the paper-templated gold structure (B). SEM images of chromatography paper (C, E), and of the paper-templated gold structure (D, F) at different magnifications. G) Cyclic voltammograms in solutions of $\text{Fe}(\text{CN})_6^{4-}$ (0.5 - 10 mM $\text{Fe}(\text{CN})_6^{4-}$ in 0.5 M KCl) recorded at 100 mV/s using a 75 mm² paper-templated gold electrode as working electrode. A platinum mesh was used as counter electrode, and a commercial Ag/AgCl electrode as reference electrode. H) Calibration line of peak current vs. concentration of $\text{Fe}(\text{CN})_6^{4-}$ for the gold paper-templated electrodes.

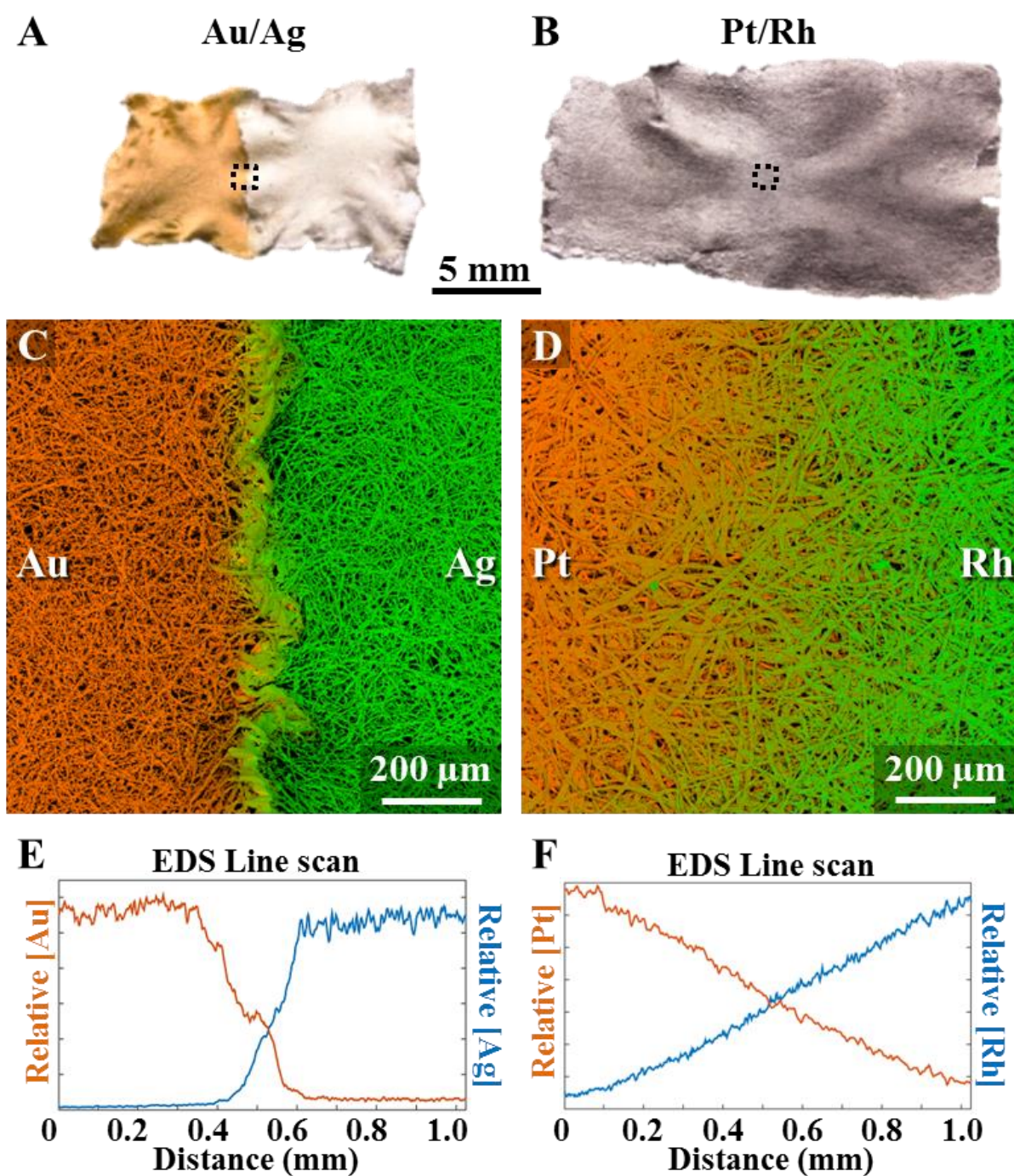


Figure 2. Photographs of the paper-templated gold/silver (A) and platinum/rhodium structures (B). EDS maps of regions (indicated in the dotted squares) of the paper-templated gold/silver (C) and platinum/rhodium structures (D). Plots indicating the relative concentration of gold and silver (E) and platinum and rhodium (F) depending on the distance from the middle of the structure; the plots were derived from the EDS maps.

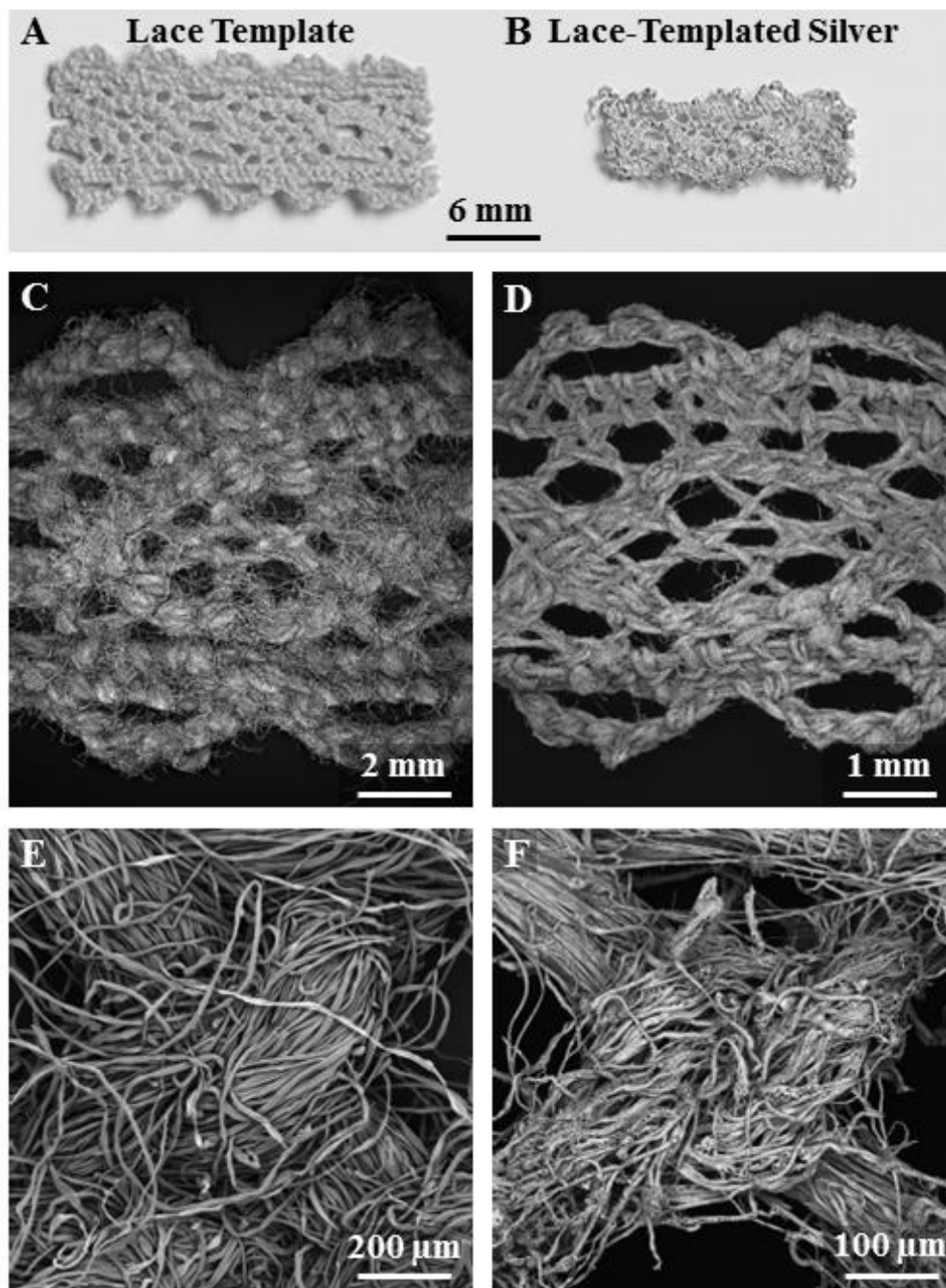


Figure 3. Photos of (A) the lace template and (B) the lace-templated silver structure. SEM images of the lace (C, E) and the lace-templated silver structure (D, F) at different magnifications.

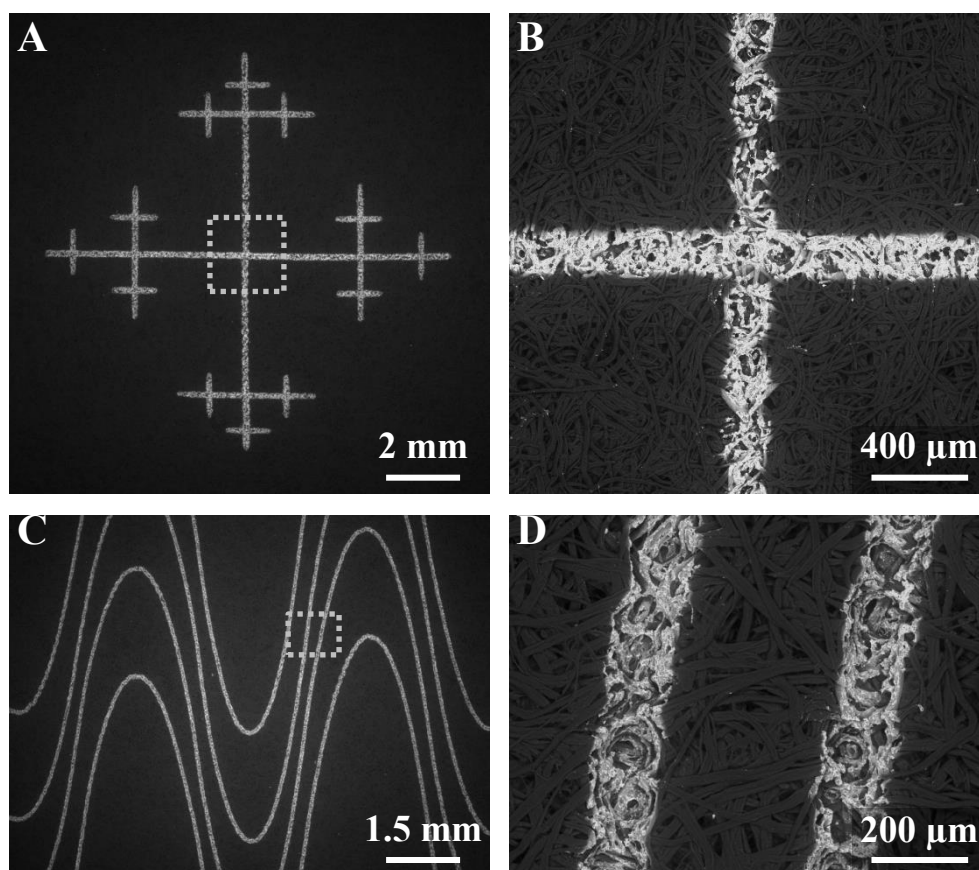


Figure 4. SEM images (A,B) of two patterns of silver wires generated on, and in, a paper substrate using a laser cutter. The EDS maps (C, D) indicate the location of elemental silver (light gray) and carbon (dark gray).

Table 1: Specific surface area of paper-templated structures and other materials

Material	Specific surface area (m ² /g)	Specific surface area (m ² /g-atom)
original paper template	1.14	-
paper-templated Au	0.24	47
paper-templated Ag	0.11	12
paper-templated Pt	0.75	146
gold foil	0.016	3.1
exfoliated graphite	84 ^[a]	1008
mesoporous alumina	365 ^[b]	37230

^[a] Value from reference [25]. ^[b] Value from reference [26]

Table 2: Composition of the paper-templated structures (composed of one noble metal element).

Paper-templated structure	Noble Metal		Oxygen		Carbon	
	mass %	atomic %	mass %	atomic %	mass %	atomic %
Au	95	55	0.9	6.6	4.1	38
Ag	95	69	2.2	10	3.2	21
Pt	97	67	0.5	4.2	2.5	29
Rh	96	78	2.0	10	1.7	12
Pd	95	74	4.0	21	0.7	5.2
Ir	95	56	2.9	18	2.5	26

Table 3: Volume resistivity of each paper-templated structure and of bulk noble metals.

Metal of Paper-templated structure	Resistivity (mΩ·mm)	Resistivity of bulk metal (mΩ·mm)^[c]
Au	39	0.022
Ag	25	0.016
Pt	82	0.104
Rh	123	0.048
Pd	360	0.105
Ir	24	0.051
Au/Ag ^[a]	21	-
Au/Ag ^[b]	372	-
Pt/Rh	724	-
Au-Pt	136	-
Ag-Pd	581	-
Au-Rd	665	-
Au-Pt-Rh	39	-

^[a] Side-by-side configuration . ^[b] Top-down configuration. ^[c] Values from reference [29]

For TOC

